

Current Drive Experiment Using Top/Outboard Side Lower Hybrid Wave Injection on TST-2 Spherical Tokamak^{*)}

Satoru YAJIMA, Yuichi TAKASE, Akira EJIRI, Naoto TSUJII, Hibiki YAMAZAKI, Charles P. MOELLER¹⁾, Takahiro SHINYA²⁾, Yuki TAKEI, Yoshiyuki TAJIRI, Yusuke YOSHIDA, Akito SATO, Akichika KITAYAMA and Naoki MATSUMOTO

The University of Tokyo, Kashiwa 277-8561, Japan

¹⁾*General Atomics, San Diego, CA 92186, USA*

²⁾*National Institute for Quantum and Radiological Science and Technology, Rokkasho 039-3212, Japan*

(Received 27 December 2017 / Accepted 3 August 2018)

In the TST-2 spherical tokamak device, we carried out a fully non-inductive current startup experiment by Landau damping of the Lower Hybrid Wave (LHW). Capacitively Coupled Combine Antennas (CCAs) were used for wave injection. The antennas are located on the outboard side and the top side of the vacuum vessel, and by reversing the toroidal magnetic field, it is possible to simulate the case of wave injection from the bottom side. The highest plasma current of 26.7 kA was achieved by top injection with the reversed toroidal magnetic field. According to numerical calculation using ray tracing and Fokker-Planck codes (GENRAY/CQL3D), the downshift of the parallel wavenumber helped the tail of the electron velocity distribution extend to higher energy than the other cases. Additionally, in order to evaluate the directionality of the wavenumber spectrum which is also important for efficient current drive, a finite element solver (COMSOL) was used. In order to avoid deterioration of the wavenumber spectrum, one limiter of the outboard antenna should be moved away toroidally by 70 mm from the current position, and the preferred distance between the antenna and the cutoff density layer is about 2 cm.

© 2018 The Japan Society of Plasma Science and Nuclear Fusion Research

Keywords: spherical tokamak, lower hybrid wave, non-inductive plasma start-up

DOI: 10.1585/pfr.13.3402114

1. Introduction

TST-2 is a spherical tokamak at the University of Tokyo, with the plasma major radius 0.36 m and minor radius 0.23 m (aspect ratio 1.6) [1, 2]. In TST-2, CCAs are used for LHW excitation [3, 4], characterized by a sharp wavenumber spectrum with peak parallel refractive index $N_{\parallel} \sim -5$. At present, there are four RF amplification systems capable of 100 kW output each. One of them is connected to the top antenna, and the output of other two are combined and connected to the outboard antenna. Typical discharge waveforms for the cases of top launch and outboard launch are shown in Fig. 1. In every case, outboard launch is initially used until the plasma current increased to at least 5 kA, because it is more difficult to form closed flux surfaces using only the top launch antenna. In TST-2, the toroidal magnetic field (TF) and the plasma current are normally in the clockwise (CW) direction as seen from the top, but by inverting the direction of the TF to the counter-clockwise (CCW) direction, propagation of the wave for top injection becomes similar to the case of bottom injection. Thus we compared both situations for top injection. Hereafter we use “Top (CW)”, “Top (CCW)”, “Outboard

(CW)” to denote the cases with different antennas and TF directions. The wavenumber upshift in the case of Top (CW) is explained in Reference [5]. Since the contribution to the parallel wavenumber is dominated by the poloidal wavenumber when the LHW wavenumber is upshifted, the upshift of the poloidal wavenumber is explained. Equation 10 in Ref. [5] expresses $dm/d\theta$ where m is the poloidal mode number, and θ is the poloidal angle. The evolution dm/dt can be evaluated using the cold plasma electrostatic dispersion relation: $D = \epsilon_{\parallel} k_{\parallel}^2 + \epsilon_{\perp} k_{\perp}^2 = 0$. We obtain $\frac{dm}{dt} \sim -\omega \left(1 + \frac{\omega_{pe}^2/\omega_{ce}^2}{\epsilon_{\perp}} \right) \frac{(r/R_0) \sin \theta}{1+(r/R_0) \cos \theta}$. The factor $-\frac{(r/R_0) \sin \theta}{1+(r/R_0) \cos \theta}$ indicates that m (≤ 0) decreases during propagation when the ray starts in the upper half region of the plasma. As a result, $|m|$ and the absolute value of the parallel wavenumber are upshifted. In the case of Top (CCW), the contribution of m to N_{\parallel} given by $\left(\frac{B_{\theta}}{B_t} \frac{m}{r} \right)$ changes sign, which corresponds to up-down reversal ($\theta \rightarrow -\theta$). The purpose of this research is to investigate the dependence of current drive characteristics on LHW injection condition.

2. Dependences on the Toroidal Field Strength

I_p and $R_{\text{mid}} I_p$ as functions of $B_{t,0}$ at R_{mid} for Top (CW), Top (CCW), and Outboard (CW) cases are shown in Fig. 2.

author's e-mail: yajima@fusion.k.u-tokyo.ac.jp

^{*)} This article is based on the presentation at the 26th International Toki Conference (ITC26).

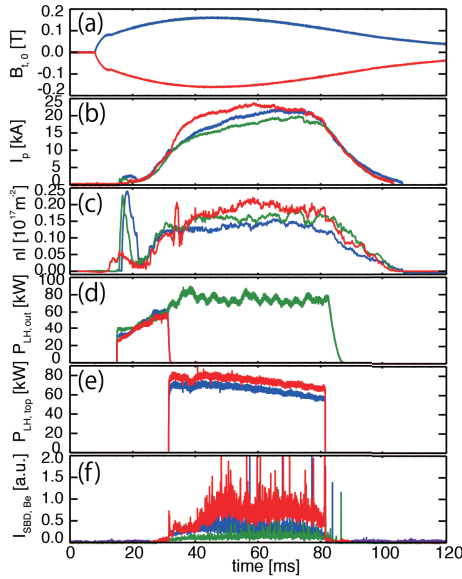


Fig. 1 Typical parameters of (a) toroidal magnetic field at the major radius of 0.38 m, (b) plasma current, (c) line-integrated plasma density (at $z = 0$ m), (d) outboard-launch power, (e) top-launch power, and (f) soft x-ray emission > 1 keV. Red, blue and green curves show the cases of Top (CCW), Top (CW), Outboard (CW), respectively.

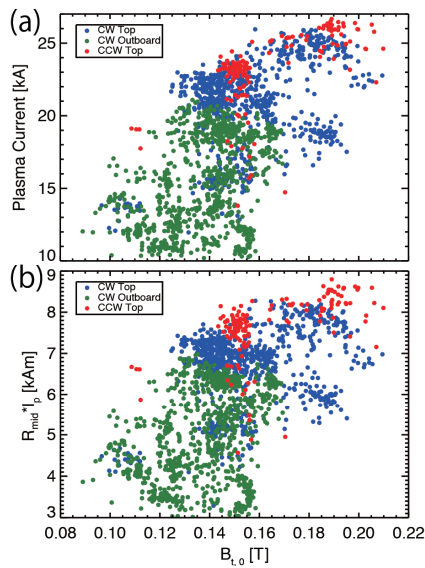


Fig. 2 Dependences of (a) plasma current, and (b) the product of plasma current and plasma major radius on the toroidal magnetic field.

Here, R_{mid} is the plasma major radius. There is a strong dependence on the toroidal magnetic field strength, and significantly higher plasma currents were obtained for both Top (CW) and Top (CCW) cases compared to Outboard (CW) case.

3. Wave Propagation Characteristics

The LHW propagations calculated by the GENRAY

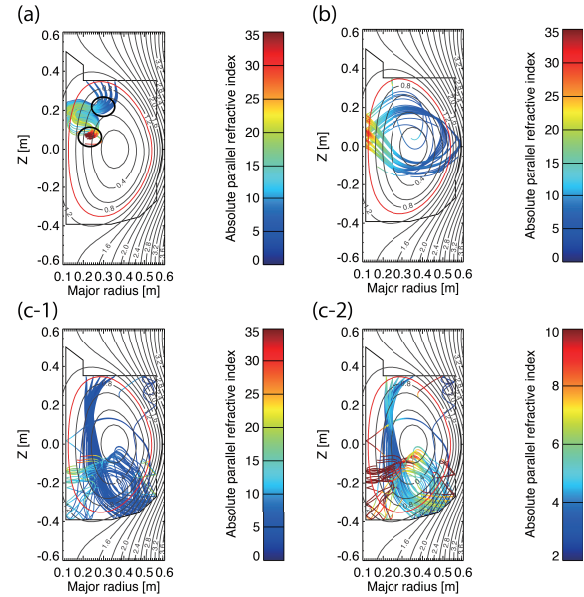


Fig. 3 Wave propagation calculated by GENRAY. (a) Top (CW) case, (b) Outboard (CW) case, and (c-1), (c-2) Top (CCW) case with two different color scales.

ray tracing code [6] is shown for different launch conditions in Fig. 3. The electron temperature (10 eV at the magnetic axis, 50 eV near the LCFS) and density ($7.2 \times 10^{17} \text{ m}^{-3}$ at the center) were measured by Thomson scattering [7], and the initial parallel wavenumber was varied (outboard: $|N_{\parallel}| = 2.7 - 9.5$, top: $|N_{\parallel}| = 1.4 - 8.7$) corresponding to the range of excited wavenumber spectra. The parallel wavenumber of the LHW injected from the outboard antenna increases in inverse proportion to the major radius due to toroidal mode number conservation. On the other hand, in the case of Top (CW), the increase in the parallel wavenumber is greatly influenced by the increased poloidal mode number. For strong wave absorption due to Landau damping in this temperature range (10 eV to 50 eV), N_{\parallel} must be increased to about 30. In the case of Top (CCW), the rays propagate downward and are reflected at the bottom limiter. After reflection, the situation becomes similar to the case of Top (CW), and the wavenumber evolutions are similar. The upshift occurs in the lower half region of the poloidal cross section. It should be noted that Figs. 3 (c-1), (c-2) show the same rays with different color ranges for the wavenumber. In Fig. 3 (a), we can see that all rays are absorbed around $\sqrt{\psi_{\text{tor}}} \sim 0.5$, where $\sqrt{\psi_{\text{tor}}}$ is the magnetic surface label parameterized and normalized by the toroidal flux. Here, we would like to discuss the absorption around $\sqrt{\psi_{\text{tor}}} \sim 0.5$. The rays propagate through this region twice [indicated by black circles in Fig. 3 (a)]. At the first pass through this region the upshift is moderate, and at the second pass the upshift is large and the rays are absorbed completely. The former moderately upshifted component contributes to extending the tail component of the distribution function to

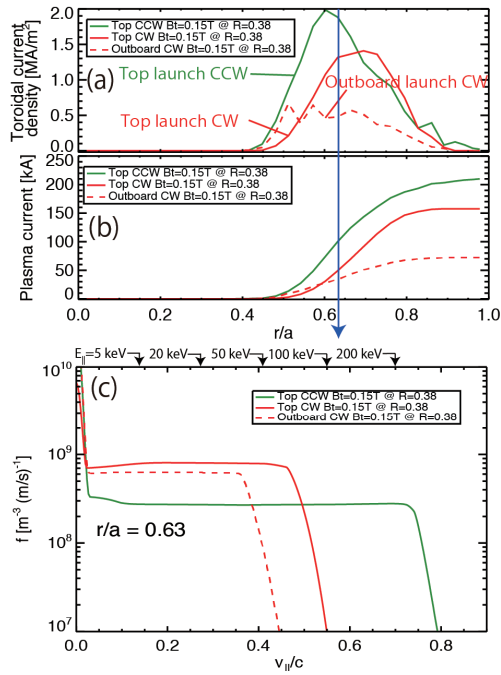


Fig. 4 (a) Plasma current density profile and (b) integrated plasma current, and (c) parallel electron velocity distribution function $f(v_{||}/c)$ at $r/a = 0.63$ obtained by GENRAY/CQL3D [8]. Note that $v_{||}/c$ corresponds to $1/N_{||}$.

high velocities, while the latter highly upshifted component is necessary to pull out the tail component from the bulk Maxwellian distribution. Regarding plasma current profile and distribution function, GENRAY/CQL3D calculation was performed (Fig. 4). As seen from Figs. 4 (a), (b), higher plasma current is driven by top-launch than by outboard-launch. Especially in the case of Top (CCW), $N_{||}$ drops below 3 during the first pass into the plasma [Fig. 3 (c-2)], which is responsible for extension of the tail to higher energies [Fig. 4 (c)].

4. Wave Excitation in the Plasma

The electromagnetic field around the antenna was calculated using COMSOL (Fig. 5). Limiters are installed to reduce the density in front of the antenna, and side walls are installed for impedance correction [see the arrows in Fig. 5 (a)]. For the outboard antenna, the parallel wavenumber spectra obtained from COMSOL calculation are shown in Fig. 6. The curves with different colors represent the toroidal mode number spectra for different densities at the limiter position (red: $1 \times 10^{16} \text{ m}^{-3}$, blue: $3 \times 10^{15} \text{ m}^{-3}$ at $R = 585 \text{ mm}$). The density decay length behind the limiter of 4 mm was used. This decay length was chosen to reproduce the transmitted power fraction of -20 dB at $1 \times 10^{16} \text{ m}^{-3}$. The calculation indicates that the wave excited from around the first element hits the limiter and is reflected as seen in Fig. 5 (b). On the other hand, if the limiter position is moved away toroidally by 70 mm, the spectral intensity of the positive wavenumber

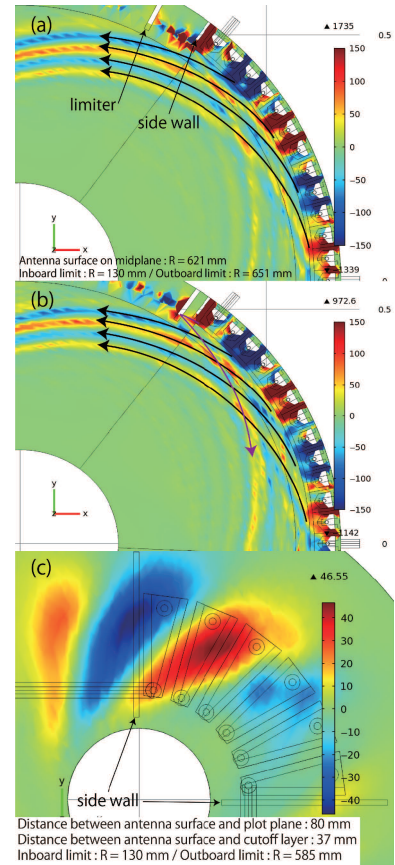


Fig. 5 Toroidal electric field on the plotting plane calculated by COMSOL [9] for the cases of (a, b) Outboard launch and (c) Top launch. Density ($1.0 \times 10^{16} \text{ m}^{-3}$) and $1/R$ dependence of the toroidal field strength is included in the cold plasma susceptibility tensor, but the magnetic field pitch angle due to the poloidal magnetic field is not included. Limiters are installed for density reduction in front of the antenna [(b) original position, (a) moved away toroidally by 70 mm], and side walls are installed for impedance correction.

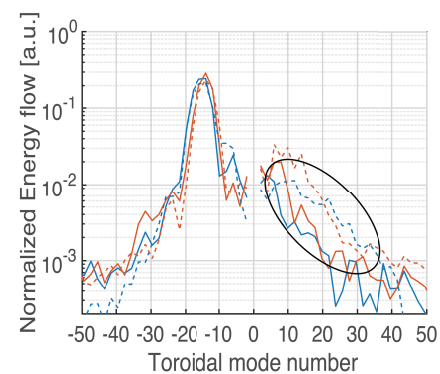


Fig. 6 Effect of wave reflection from the limiter for outboard launch calculated by COMSOL. Dashed (solid) lines show the radial energy flow spectrum calculated for the current limiter position (for the case with the limiter moved away toroidally by 70 mm). Toroidal mode number n_t of the 200 MHz LHW can be expressed as $n_t \approx \frac{2\pi}{1.5} N_{||} R$ near the edge, where R is the major radius.

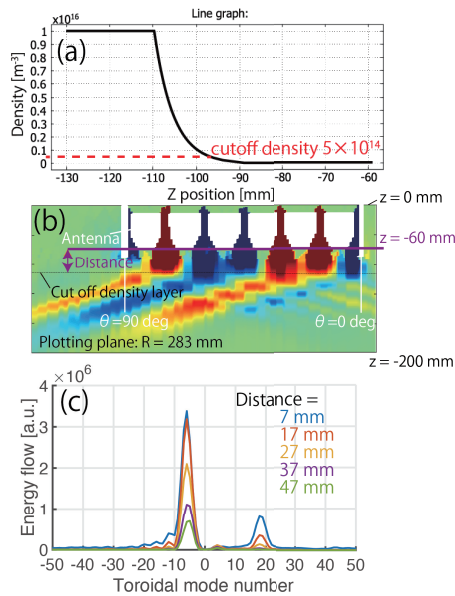


Fig. 7 Effect of the antenna-cutoff distance on the excited wave spectrum for Top launch calculated by COMSOL. (a) density profile in the vertical direction, (b) antenna-cutoff distance, and (c) excited toroidal mode number spectrum of vertical energy flow.

is reduced to one third or less at densities of $1 \times 10^{16} \text{ m}^{-3}$ and $3 \times 10^{15} \text{ m}^{-3}$. For the top antenna [Fig. 5 (c)], the limiters are 150 mm away from the antenna elements, so the reflection from the limiter described above is not important and is not included in the calculation. Instead, the antenna-cutoff affects the wavenumber spectrum (Fig. 7). In the calculation, the antenna-cutoff distance was scanned in the range 7–47 mm. When this distance approaches 27 mm, a spectral component with large wavenumber appears in the opposite (positive) direction. This is due to excessively enhanced antenna-plasma coupling. Although the power flow to the plasma increases, when the antenna-cutoff distance becomes close to 17 mm, the main spectral component (toroidal mode number ~ 8) becomes saturated, but the spectral component in the opposite direction keeps increasing. For Outboard (CW) case this effect is not important because the plasma often becomes inboard limited due

to the increase of the vertical magnetic field during current ramp up and the antenna-cutoff distance becomes larger.

5. Summary

The experimental result indicates that the current driven by the LHW has a strong positive correlation with the toroidal magnetic field strength, and both Top (CW) and Top (CCW) cases achieve higher currents than Outboard (CW) case. According to GENRAY/CQL3D calculation, top-launch LHW eventually causes a significant increase in the parallel wavenumber. Additionally, in the case of Top (CCW), the wave initially propagates through the plasma with reduced wavenumber, which is considered to help extend the tail of the velocity distribution function to higher energies. Using COMSOL we found that there exists a suitable antenna-cutoff distance for the top launch antenna. In addition, the limiter position of the outboard launch antenna should be moved away sufficiently to reduce the counter-driving component.

Acknowledgement

This work was supported by JSPS Grant-in-Aid for Scientific Research 21226021 and 23360409, NIFS Collaboration Research Program NIFS10KOAR012, JSPS A3 Foresight Program 'Innovative Tokamak Plasma Startup and Current Drive in Spherical Torus, and NINS program of Promoting Research by Networking among Institutions (Grant Number 01411702).

- [1] Y. Takase *et al.*, Nucl. Fusion **41**, 1543 (2001).
- [2] Y. Takase *et al.*, Nucl. Fusion **53**, 063006 (2013).
- [3] T. Shinya *et al.*, Nucl. Fusion **55**, 073003 (2015).
- [4] T. Shinya *et al.*, Nucl. Fusion **57**, 036006 (2017).
- [5] P.T. Bonoli *et al.*, Phys. Fluids **25**(2), 359 (1982).
- [6] A.P. Smirnov *et al.*, 1994 GENRAY Code
www.compxco.com/genray.html
- [7] N. Tsujii *et al.*, EPJ Web of Conferences **157**, 02009 (2017).
- [8] R.W. Harvey *et al.*, 1985 CQL3D Code
www.compxco.com/genray.html
- [9] COMSOL Multiphysics Home Page
<https://www.comsol.eu/>